Burst Mode Hybrid Spread Spectrum Technology for Covert Acoustic Communication

Yanling Yin, Feng Zhou, Gang Qiao, Songzuo Liu, Yang Yu
Science and Technology on Underwater Acoustic Laboratory
Harbin Engineering University
Harbin China
zhoufeng@herbeu.edu.cn

***Abstract* — To overcome the problem of underwater transmitted platform being detected by energy detector, a burst hybrid spread spectrum scheme which transmits extremely short signal for covert underwater acoustic communication is proposed in this paper. A non-data-aided self-synchronization algorithm is achieved using a time-frequency 2-dimensional search algorithm, carrier frequency offset and symbol offset forms a two-dimensional phase space. In the two-dimensional phase space, optimal carrier frequency and chip phase are found at the same time. An orthogonal-hybrid spread spectrum communication scheme with direct sequence spread spectrum (DSSS)-BPSK modulation, Cyclic Shift Keying (CSK) modulation and DSSS-MFSK modulation is proposed which promotes the bandwidth efficiency. The non-coherent maximum likelihood receiver is adopted to counteract the fast selected and frequency selected channel fading. The performance of the system over AWGN channel and underwater acoustic multipath channel is analyzed through the theory analysis and numerical simulation. The data from the shallow water experiment near South Sea, China, is used to demonstrate the system performance. The results from the experiment showed that the data rate can achieve up to 317 bps and bit error rate (BER) under 10^{-3} in the distance of 5 km over the bandwidth of 4 kHz.**

Keywords—burst-mode communication; hybrid spread spectrum; covert communication; orthogonal modulation

I. INTRODUCTION

To realize the low probability of detection (LPD) in underwater acoustic communication, the most commonly used method is the DSSS method. The DSSS method usually adopts rake receiver and space diversity to promote the receive signal-to-noise ratio (SNR) and to minimize the probability of detection and interception [1-2]. Although the DSSS will not likely be detected by a commonly used energy detector by using the long code sequence, it can still be detected by a frequency detector for its fixed carrier frequency. In the base of the DSSS, the frequency hopping modulation uses pseudorandom sequence to control the carrier frequency changing periodically. So it is hard to detect the hopping pattern and the detection probability is reduced. Whereas, the bandwidth efficiency of the frequency hopping modulation is low [3-4]. Recently, the multicarrier spread spectrum approach is used for covert communication. The error correction code and channel equalization technology are applied in the scheme to promote the system's robustness. The long code sequence is still necessary to realize the covert communication [5-6].

The covert acoustic communication methods mentioned above all send the signal continuously which can still be detected by energy integration over a long period time. To overcome the problem, a burst mode hybrid spread spectrum scheme for covert acoustic communication is proposed in this paper. The scheme transmits impulse signals randomly in time-domain and controls the impulse length within 100ms. Due to its short signal length, it is hard to be detected by energy detector in time-domain. So the burst mode communication scheme promotes the probability of detection and interception.

In the radio frequency communications, the typical burst format for data packet uses preamble for carrier and symbol timing recovery [7]. The preamble doesn't carrier information which reduces the transmission efficiency and increases the impulse length. The data packet of the scheme proposed in the paper is structured without preamble and uses one of the data channels to realize the synchronization. In the hybrid signal, the inphase branch is modulated by BPSK-DSSS and is used as the synchronization channel. The quadrature branch is modulated by CSK. In order to promote the data rate, another channel is modulated by MFSK-DSSS is added in the hybrid signal.

The paper is organized as follows. Section II describes the system's transmitter and receiver structure. The synchronization method is introduced and the performance of the system in AWGN channel and underwater acoustic multipath channel is analyzed in this part. Section III presents the performance of the system in different channels through simulation and sea trail. The last part is conclusion.

II. MODEL SYSTEM

A. Transmitter

The transmitter diagram of the considered system is shown in Fig.1. Group the input data stream into $1+k_0+k_1$ bits with symbol duration T_s, where BPSK modulation carriers 1 bit, CSK modulation carries k_0 bits and MFSK modulation carriers k_1 bits. BPSK modulates by $\cos(2\pi f_c t)$, CSK modulates by $\sin(2\pi f_c t)$, the frequency tones of the MFSK signal is

This work was supported by the National Natural Science Foundation of China under Grant No. 1127407, National High Technology Research and Development Program of China under Grant No. 2009AA093601-2 and the Underwater Acoustic Technology Laboratory Foundation of China under Grant No. 9140C200801110C2004.

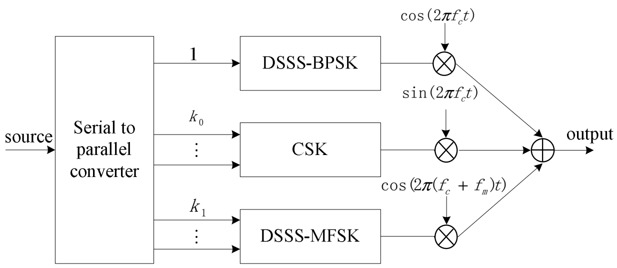

Fig. 1. Transmitter block diagram of burst mode hybrid spread spectrum system

modulated at frequencies of $f_c + m\Delta(m = 1,2,...,M)$ with $\Delta = i / T_s, i = 1,2,...$, i controls the frequency space of different tones. The carrier frequencies of three signals are orthogonal over the information symbol duration. The transmitted symbols are spread with different m-sequences containing N chips yielding a theoretical processing gain of 18dB at the receiver. The chip duration is assumed to be T_c, i.e., $T_s = NT_c$. The modulated spreading sequence by CSK can be shown as follows

$$c^k(t) = \begin{cases} c(t + k\Delta\tau) & (0 \le t \le T_s - k\Delta\tau) \\ c(t - T_s + k\Delta\tau) & (T_s - k\Delta\tau < t \le T_s) \end{cases} \tag{1}$$

Where k represents the information modulated by CSK and $c(t)$ is the spreading wave chip. For traditional M-ary frequency shift keying (MFSK) modulation, the modulation frequency tones are not overlapped, so the bandwidth efficiency is low. Whereas, if the adjacent frequency tones are minimized to make the carriers be orthogonal, there is still no inter-carrier interference, while the bandwidth efficiency is promoted significantly. The orthogonal frequency space is treated as the minimal frequency space. The orthogonal frequency space of MFSK modulation before direct-sequence (DS) spectrum spreading is $1/T_s$ and it is $1/T_c$ after DS spectrum spreading. On the other hand, if the frequency space of the MFSK DS system is $1/T_s$, this means that there is a strong spectral overlap of the different frequency tones after DS spectrum spreading, which increases the inter-carrier interference, however, different MFSK tones are still orthogonal over the symbol duration [8]. That means the signal associated with each MFSK tones can be recovered, as long as the channel does not violate the condition.

As shown in Figs.2 and 3, there are the frequency spectrums with MFSK modulation before DS spectrum spreading and after DS spectrum spreading with the frequency space $1/T_s$. To reduce the interference caused by multipath, we can increase the frequency space. Assume the frequency space is $\Delta = \lambda / T_s$, where λ is normalized frequency space, we can adjust λ to change the frequency space [9].

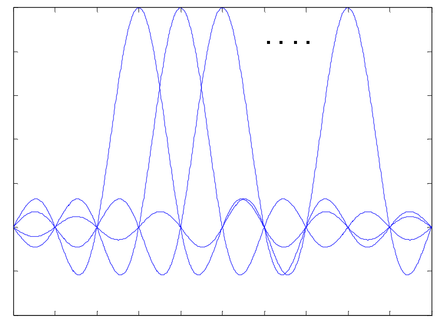

Fig. 2. Frequency spectrum before DS spectrum spreading with MFSK modulation

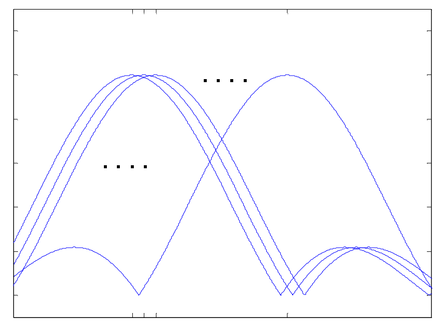

Fig. 3. Frequency spectrum after DS spectrum spreading with MFSK modulation

The inphase branch is as the pilot channel for the traditional CSK spread spectrum system and the system's bandwidth efficiency is $k_0 / 2N$, where N is the spectrum spreading gain. The inphase branch of the proposed system in the paper is modulated by BPSK and is as the pilot channel at the same time; meanwhile, another channel whose modulation frequency is orthogonal with other channels modulated by MFSK is transmitted together. The bandwidth efficiency of the hybrid system is $(1 + k_0 + k_1) / 2N$. Compared to the traditional CSK spread spectrum system, the hybrid system promotes the bandwidth efficiency.

B. *System Synchronization*

Synchronization plays a critical role for a more accurate replica of the transmitted symbol sequence in a receiver design. Synchronization mainly contains carrier synchronization and time synchronization, meanwhile, the carrier synchronization contains carrier frequency synchronization and carrier phase synchronization. The typical data packet uses a preamble for carrier and symbol timing recovery, while, for the complex multipath underwater acoustic channel, a long preamble is needed to capture the signal which decreases the

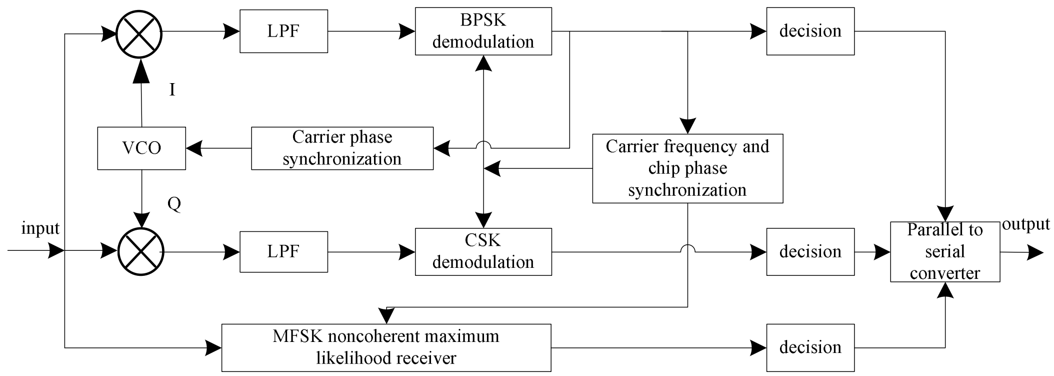

Fig. 4. Receiver block diagram of the burst-mode hybrid spread spectrum system

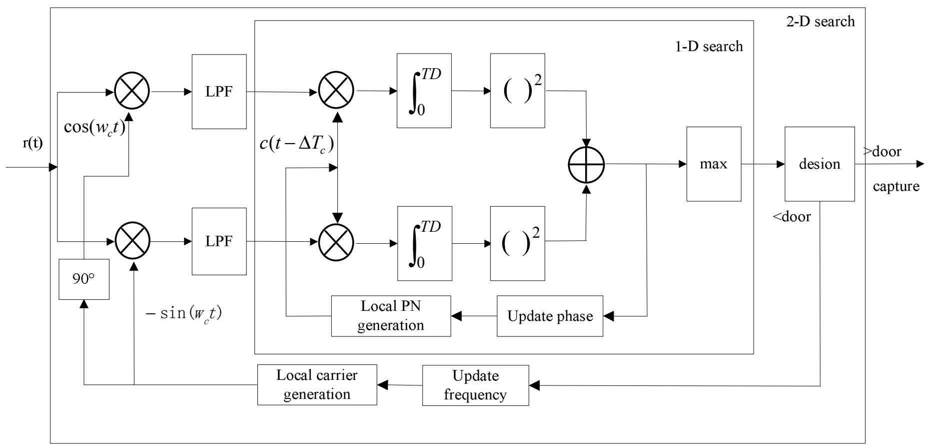

Fig. 5. Block diagram of the time-frequency 2-dimensional search algorithm

transmission efficiency. A non-data-aided self-synchronization algorithm is adopted in the paper. The algorithm is introduced as follows.

For the transmitter as depicted above, the transmitted signal can be written as

$$s(t)=\sqrt{2P}\Big(b_0(t)c_0(t)\cos(2\pi f_c t)+c_1^{(b_1(t))}(t)\sin(2\pi f_c t)+c_2(t)\cos\big(2\pi\big(f_c+\Delta b_2(t)\big)t+\varphi_m\big)\Big) \tag{2}$$

Where f_c is the carrier frequency and P is the power of the transmitted signal. Assume the carrier phase is zero and φ_m is the phase introduced by the mth FSK modulator. $b_0(t)$ and $b_2(t)$ are the bits modulate by BPSK and MFSK. $b_0(t)$ takes the values -1 or +1, for the information sequence is M_1-ary, $b_2(t)$ takes the values from the set $\{1-M_1,3-M_1,...,-1,1,...,M_1-3,M_1-1\}$ with the equal probability. Δ is the frequency space. $c_0(t)$, $c_1(t)$ and $c_2(t)$ is chip waveform of the BPSK modulation, CSK modulation and MFSK modulation. $c_1^{(b_1(t))}$ represents the $c_1(t)$ circles shift with the information $b_1(t)$ modulated by CSK. The frequencies of three data channels are orthogonal. Considering that the transmitted signal passes through the AWGN channel, the receive signal can be expressed as

$$\begin{aligned} r(t)=\sqrt{2P}\Big(&b_0(t-\tau)c_0(t-\tau)\cos\big(2\pi(f_c+f_d)t+\varphi\big)\\ &+c_1^{(b_1(t))}(t-\tau)\sin\big(2\pi(f_c+f_d)_c t+\varphi\big)\\ &+c_2(t-\tau)\cos\big(2\pi\big(f_c+\Delta b_2(t-\tau)+f_d\big)t\big)+\varphi'\Big)+n(t) \end{aligned} \tag{3}$$

Where τ represents the time delay and f_d represents Doppler shift. $\varphi=\varphi_0+2\pi(f_c+f_d)\tau$ and $\varphi'=\varphi_m+\varphi_0+2\pi\big(f_c+f_d+\Delta\cdot b_2(t-\tau)\big)\tau$ is the difference between the transmitter phase and the receiver phase. φ_0 is the random carrier phase distributed uniformly over $(0,2\pi]$. While $n(t)$ represents the additive white Gaussian noise (AWGN) with zero mean and double-sided power spectral density of $N_0/2$. The receiver block diagram of the considered system is shown in Fig.4. Before demodulation, the signal capture is needed. According to the character of the three channel signals, the channel modulated by BPSK is used

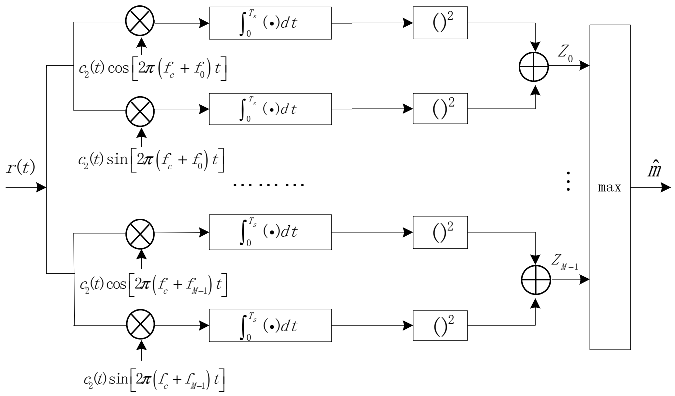

Fig. 6. Non-coherent maximum likelihood receiver with MFSK demodulation

as the synchronization channel. A time-frequency 2-dimensional search algorithm is used to capture the signal [10].

The carrier frequency offset and the symbol offset form a two-dimensional phase space. In the space, optimal carrier frequency and chip phase are found at the same time (the detail please refers to the literature [10]). The block diagram of the time-frequency 2-dimensional search algorithm is shown in Fig. 5.

After the perfect synchronization, the non-coherent maximum likelihood receiver is adopted for CSK and MFSK demodulation. The receiver with MFSK demodulation is shown in Fig.6. The CSK non-coherent demodulation is similar to the MFSK demodulation. The only difference is that the receiver multiplies the different cycle shift of $c_1(t)$ replacing of the different frequency carrier.

The BPSK demodulation maybe has a $\pm\pi$ phase error caused by carrier phase offset. So the accurate carrier phase estimation is needed before demodulation. It can be estimated by the signal modulated by BPSK. The carrier frequency and chip phase are assumed to be perfect estimates. Consequently, the inphase branch can be expressed as

$$\begin{aligned}I(t)&=LPF\left(r(t)\cos\left(2\pi\left(f_c+f_d\right)(t-\tau)\right)\right)\\&=b_0(t)c_0(t)\cos(\varphi_0)-c_1^{(b_1(t))}(t)\sin(\varphi_0)\\&\quad+c_2(t)\delta\left(b_2(t),m\right)\cos(\varphi_0')+n_I'(t)\end{aligned}\tag{4}$$

The quadrature branch is expressed as

$$\begin{aligned}Q(t)&=LPF\left(r(t)\sin\left(2\pi\left(f_c+f_d\right)(t-\tau)\right)\right)\\&=-b_0(t)c_0(t)\sin(\varphi_0)\\&\quad+c_1^{(b_1(t))}(t)\cos(\varphi_0)-c_2(t)\delta\left(b_2(t),m\right)\sin(\varphi_0')\\&\quad+n_Q'(t)\end{aligned}\tag{5}$$

Where $\varphi_0'=\varphi_0+\varphi_m$, $n_I'(t)$ and $n_Q'(t)$ are contributed by $n(t)$ of (3). $\delta\left(b_2(t),m\right)=1$ for $b_2(t)=m$, otherwise $\delta\left(b_2(t),m\right)=0$ and m is the symbol information modulated by MFSK. Multiply $I(t)$ and $Q(t)$ by the chip $c_0(t)$ and integrate the results, we can have

$$\begin{aligned}I'&=\frac{1}{T_s}\int_0^{T_s}I(t)c_0(t)dt\\&=b_0\cos(\varphi_0)\frac{1}{T_s}\int_0^{T_s}c_0(t)c_0(t)dt\\&\quad-\sin(\varphi_0)\frac{1}{T_s}\int_0^{T_s}c_1^{(b_1(t))}(t)c_0(t)dt\\&\quad+\delta(b_2,m)\cos(\varphi_0)\frac{1}{T_s}\int_0^{T_s}c_2(t)c_0(t)dt\\&\quad+\frac{1}{T_s}\int_0^{T_s}n_I'(t)dt\\&=b_0\cos(\varphi_0)-\sin(\varphi_0)R\left(c_0,c_1^{(b_1)}\right)\\&\quad+\delta(b_2,m)\cos(\varphi_0)R(c_0,c_2)+N_I'\\&=b_0\cos(\varphi_0)+N_I''\end{aligned}\tag{6}$$

$$\begin{aligned}Q'&=\frac{1}{T_s}\int_0^{T_s}Q(t)c_0(t)dt\\&=-b_0\sin(\varphi_0)\frac{1}{T_s}\int_0^{T_s}c_0(t)c_0(t)dt\\&\quad+\cos(\varphi_0)\frac{1}{T_s}\int_0^{T_s}c_1^{(b_1(t))}(t)c_0(t)dt\\&\quad-\delta(b_2,m)\sin(\varphi_0)\frac{1}{T_s}\int_0^{T_s}c_2(t)c_0(t)dt\\&\quad+\frac{1}{T_s}\int_0^{T_s}n_Q'(t)dt\\&=-b_0\sin(\varphi_0)+\cos(\varphi_0)R\left(c_0,c_1^{(b_1)}\right)\\&\quad-\delta(b_2,m)\sin(\varphi_0)R(c_0,c_2)+N_Q'\\&=-b_0\sin(\varphi_0)+N_Q''\end{aligned}\tag{7}$$

Where $R\left(c_0,c_1^{(b_1)}\right)$ represents the cross-correlation value between $c(t)$ and $c_1^{(b_1(t))}(t)$. $R(c_0,c_2)$ represents the cross-correlation value between $c_0(t)$ and $c_2(t)$. N_I'' and N_Q'' are contributed by $n(t)$ and the interference of other channels. The cross-correlation value is very small for the orthogonality of the codes. So the carrier phase can be estimated as

$$\hat{\varphi}_0=-\tan^{-1}\left(\frac{Q'}{I'}\right)\tag{8}$$

C. *Performance Analysis*

Considering the AWGN channel it can be assumed that the receiver acquires perfect synchronization. Because the carrier frequency of each channel is orthogonal, there is no interference caused by other channels after bringing the signal down to the baseband. So the BER of each channel is the same as the BER of the signal modulated alone. Assuming the BER of the BPSK modulation, CSK modulation and MFSK modulation are P_0 , P_1 and P_2 , the binary information 0 and 1 has the equal probability. The total BER of the system can be expressed as

$$P_e = \frac{P_0 + k_0 P_1 + k_1 P_2}{1 + k_0 + k_1} \tag{9}$$

Regardless of the additive noise, the signal passes through the time-invariant acoustic multipath channel and the received signal can be expressed as

$$\begin{aligned} r(t) = \sqrt{2P} \sum_{l=1}^{L} \alpha_l \Big[& \big(b_0 (t-\tau_l) c_0 (t-\tau_l) \\ & \times \cos\big(2\pi f_c (t-\tau_l) + \phi_l\big)\big) \\ & + c_1^{(b_1(t))} (t-\tau_l) \sin\big(2\pi f_c (t-\tau_l) + \phi_l\big) \\ & + c_2 (t-\tau_l) \cos\big(2\pi \big(f_c + \Delta b_2 (t-\tau_l)\big)(t-\tau_l)\big) + \varphi_m + \phi_l \Big] \end{aligned} \tag{10}$$

Where α_l , τ_l and ϕ_l represent the attenuation factor, delay and phase-shift for the multipath component of the channel, L is the total number of the diversity paths. We choose BPSK signal as an example to analyze the influence of demodulation over the multipath channel. Let us assume that the received signal synchronizes the first arrived ray which has the maximum energy. So the corresponding time delay is zero. Assume that the first BPSK transmitted data bit is $b_0[0]$ and the former data bit is $b_0[-1]$, the decision variable Z corresponding to the first bit can be expressed as

$$Z = \frac{1}{T_s} \int_0^{T_s} r(t) c_0 (t) \cos(2\pi f_c t)\, dt \tag{11}$$

Upon substituting (10) into (11), Z can be written as

$$\begin{aligned} Z = \sqrt{\frac{P}{2}} \Big\{ & \delta(b_0[0], k) \\ & + \sum_{l=2}^{L} \frac{1}{T_s} \int_0^{T_s} \alpha_l b_0 (t-\tau_l) c_0 (t-\tau_l) c_0 (t) \cos(2\pi f_c \tau_l + \phi_l)\, dt \\ & + \sum_{l=2}^{L} \frac{1}{T_s} \int_0^{T_s} -\alpha_l c_1^{(b_1(t))} (t-\tau_l) c_0 (t) \sin(2\pi f_c \tau_l + \phi_l)\, dt \\ & + \Big[\sum_{l=2}^{L} \frac{1}{T_s} \int_0^{T_s} \alpha_l c_1 (t-\tau_l) c_0 (t) \\ & \times \cos\big(2\pi \big(f_c + \Delta b_2 (t-\tau_l)\big) \tau_l + \varphi_m + \phi_l\big)\, dt \Big] \Big\} \\ = D + & \sum_{l=2}^{L} I_s (l) + \sum_{l=2}^{L} I_{M1} (l) + \sum_{l=2}^{L} I_{M2} (l) \end{aligned} \tag{12}$$

Where D in (12) is the desired output which can be written as $D = \delta(b_0[0], k)$. K is the binary information modulated by BPSK takes values of -1 or +1. There are three types interference in (12). The interference term of $I_s(l)$ is contributed by the path $l, l = 1, 2, ..., L-1$ associated with the same data channel, which can be expressed as

$$\begin{aligned} I_s (l) = & \frac{1}{T_s} \int_0^{\tau_l} \alpha_l b_0 [-1] c_0 (t) c_0 (t-\tau_l) \cos(\theta_l)\, dt \\ & + \frac{1}{T_s} \int_{\tau_l}^{T_s} \alpha_l b_0 [0] c_0 (t) c_0 (t-\tau_l) \cos(\theta_l)\, dt \\ = & \alpha_l \cos(\theta_l) \big(b_0[-1] R_{c_0,c_0} [\tau_l] + b_0[0] \hat{R}_{c_0,c_0} [\tau_l] \big) \end{aligned} \tag{13}$$

Where $\theta_l = \phi_l + 2\pi f_c \tau_l$, which is a random variable uniformly distributed in $(0, 2\pi]$, while $R_{c_0,c_0}[\tau_l]$ and $\hat{R}_{c_0,c_0}[\tau_l]$ are partial auto-correlation functions, which are defined as

$$R_{c_0,c_0} [\tau_l] = \frac{1}{T_s} \int_0^{\tau_l} c_0 (t) c_0 (t-\tau_l)\, dt \tag{14}$$

$$\hat{R}_{c_0,c_0} [\tau_l] = \frac{1}{T_s} \int_{\tau_l}^{T_s} c_0 (t) c_0 (t-\tau_l)\, dt \tag{15}$$

The interference term of $I_{M1}(l)$ is contributed by the path $l, l = 1, 2, ..., L-1$, induced by CSK modulation channel, which can be expressed as

$$\begin{aligned} I_{M1} (l) = & \frac{1}{T_s} \int_0^{\tau_l} -\alpha_l b_0 [-1] c_0 (t) c_1^{b_1[-1]} (t-\tau_l) \sin(\theta_l)\, dt \\ & + \frac{1}{T_s} \int_{\tau_l}^{T_s} -\alpha_l b_0 [0] c_0 (t) c_1^{b_1[0]} (t-\tau_l) \sin(\theta_l)\, dt \\ = & \alpha_l \sin(\theta_l) b_0[-1] R_{c_0,c_1} \big[\tau_l, b_1[-1]\big] \\ & + \alpha_l \sin(\theta_l) b_0[0] \hat{R}_{c_0,c_1} \big[\tau_l, b_1[-1]\big] \end{aligned} \tag{16}$$

Where $R_{c_0,c_1}\big[\tau_l, b_1[-1]\big]$ and $\hat{R}_{c_0,c_1}\big[\tau_l, b_1[-1]\big]$ are partial cross-correlation functions of $c_0(t)$ and $c_1(t)$. $c_1^{b_1[-1]}(t)$ represents the chip waveform modulated by the bit $b_0[-1]$. The interference term of $I_{M2}(l)$ is contributed by the path $l, l = 1, 2, ..., L-1$ induced by MFSK modulation channel, which can be expressed as

$$\begin{aligned} I_{M2} (l) = & \Big(\frac{1}{T_s} \int_0^{\tau_l} \alpha_l b_0 [-1] c_0 (t) c_2 (t-\tau_l) \\ & \times \cos\big(2\pi \big(f_c + \Delta b_2 [-1]\big) \tau_l + \varphi_m [-1] + \phi_l\big)\, dt \Big) \\ & + \Big(\frac{1}{T_s} \int_{\tau_l}^{T_s} \alpha_l b_0 [0] c_0 (t) c_2 (t-\tau_l) \\ & \times \cos\big(2\pi \big(f_c + \Delta b_2 [0]\big) \tau_l + \varphi_m [0] + \phi_l\big)\, dt \Big) \\ = & \alpha_l b_0[-1] R_{c_0,c_2} \big[\tau_l, b_2[-1], \theta_m[-1]\big] \\ & + \alpha_l b_0[0] \hat{R}_{c_0,c_2} \big[\tau_l, b_2[0], \theta_m[0]\big] \end{aligned} \tag{17}$$

Where $\theta_m = \varphi_m + \phi_l + 2\pi f_c \tau_l$, $R_{c_0,c_2}\left[\tau_l, b_2[-1], \theta_m[-1]\right]$ and $\hat{R}_{c_0,c_2}\left[\tau_l, b_2[0], \theta_m[0]\right]$ are partial cross-correlation functions of $c_0(t)$ and $c_2(t)$. Having analyzed the interference terms in (12), we can found that they have an important relationship with the correlation of the chip waveform. The auto-correlation of the m sequence with the chip duration T_c can be written as

$$R_N(\tau) = \begin{cases} 1 - \dfrac{N+1}{N}\dfrac{|\tau|}{T_c} & |\tau| \le T_c \\ -\dfrac{1}{N} & |\tau| > T_c \end{cases} \tag{18}$$

From the formula, we can see that the auto-correlation value goes down to $-1/N$ with the time delay over the chip duration. So the interference caused by the same data channel is very small. The other two interference terms have an important relationship with the cross-correlation of the DS spectrum spreading sequence. Assume the DS spectrum spreading sequence $c_0(t)$ and an arbitrary sequence $c(t)$ has a same value with the number of $\mathrm{S}\left(\mathrm{S}\in\{1,2,..,\mathrm{N}\}\right)$ chips and a different value with the number of N-S chips, the cross-correlation can be expressed as

$$R_{c_0c_1}(\tau) = \frac{1}{T_s}\int_0^{T_s} c_0(t)c_1(t)\,dt = \frac{2S-N}{N} \tag{19}$$

We have analyzed the performance of the BPSK coherent demodulation over the multipath channel above, the non-coherent demodulation of CSK and MFSK is similar to BPSK. Here a detailed analysis is not given. The performance of the system will be numerically evaluated as follows.

III. NUMERICAL AND EXPERIMENTAL RESULTS

A. Numerical Simulation

In the simulation, the sample rate is set to 48 kHz and the carrier frequency is set to 6 kHz. The DS spreading sequence is m sequence with the length of 63. CSK modulation carries 5 bits and MFSK modulation carriers 3 bits whose carrier frequency space is $1/T_s$ .The total bandwidth is 4.2 kHz and the data rate is 285.7 bps. A burst frame contains 3 symbols. The length of the burst frame is 94.5 ms.

Fig.7 and Fig.8 show each data channel and the hybrid system's BER performance for different SNR over the AWGN channel and multipath channel. Each data channel has the same E_b/N_0 . The channel model uses 5 discrete paths, with the normalized amplitudes 1, 0.4, 0.3, 0.2, 0.15 and the channel delay 0, 3.1, 8.3, 14.6, 18.7 ms. From the figures we can see that the performance of the CSK modulation is best and the MFSK is worst. The performance of the hybrid system is close to the BPSK modulation. Due to the interferences caused by multipath, the performance over the multipath channel is worse than that over the AWGN channel.

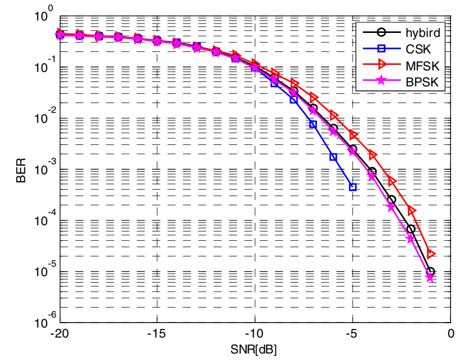

Fig. 7. the system's BER over the AWGN channel

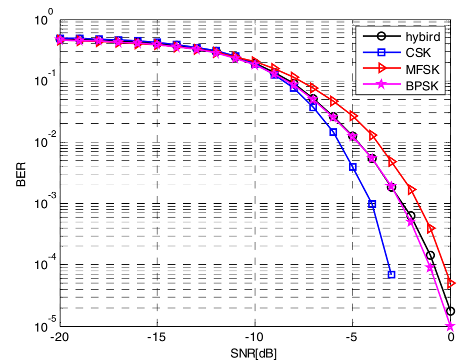

Fig. 8. the system's BER over the multipath channel

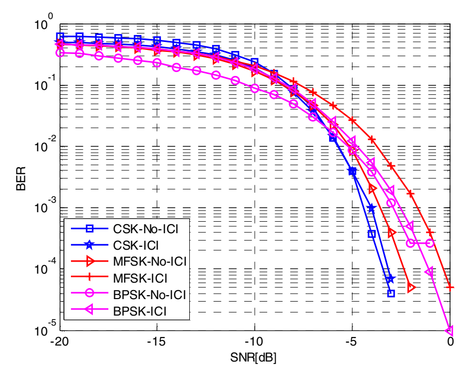

Fig. 9. BER comparison over the multipath channel

In order to obverse the interference caused by other data channels, we let only one branch of the hybrid signal pass through the multipath channel. So there is only the multipath interference caused by the same data channel expressed as in equation (13). According to the expression (9) we can calculate the hybrid system's BER i.e. the BER without interferences caused by other data channels. We define this BER as a theory BER. We keep each data channel has the same transmitted power in two different simulation. The results are compared in Fig. 9. We use XX-No-ICI to represent the BER that each modulated signal passes through the multipath channel alone and XX-ICI to represent the hybrid system's BER. From the figure we can clearly see the interferences of each data channel.

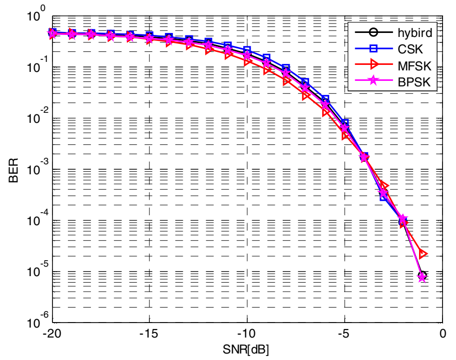

Fig. 10. BER comparison after adjust transmitted power over the multipath channel

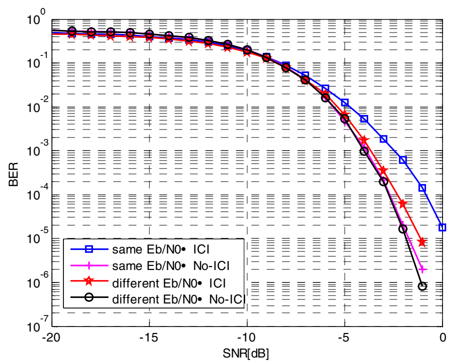

Fig. 11. The hybrid system's BER comparison after adjust the transmitted power

The interference of CSK and BPSK modulation caused by other data channels is smaller while the MFSK is larger.

From Figs.7 - 9, we can find that there is a little difference of the BER performance among the three signals. CSK modulation performs best. MFSK modulation performs worst and is affected by multipath severely. So we can enhance the transmitted power of the MFSK signal appropriately to make the performance be close to each other. The hybrid system's BER performance will be improved. After adjusting the transmitted power, the BER performance for different SNR is shown in Fig.10. As shown in Fig.10, the performance is close to each other and the performance after adjusting the transmitted power is improved compared to the system with equal E_b / N_0. In order to see it clearly, we replot the hybrid system's BER performance with ICI and without ICI in Fig.11. From the figure we can clearly see that the BER after adjusting the transmitted power is lower and is close to the theory BER.

B. *Exprimental Results*

The sea experiments were conducted in the South Sea China, in April 2013. The water depth in the experimental area is about 50 m. The sound speed profile presented faint negative grads. The fixed source was located at about 25 m and the received hydrophone was located at about 15 m. The system's bandwidth was 4 kHz ~ 8 kHz. Measured channel impulse response using LFM signal in the distance of 5km is shown in

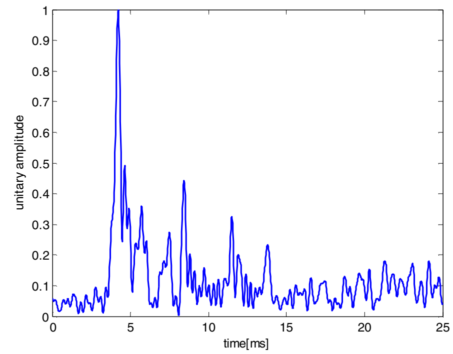

Fig. 12. channel impulse response

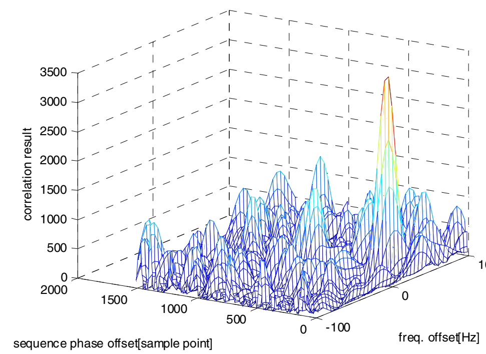

Fig. 13. time-frequency 2D search relation figure

Fig.12. There are about 7 paths and the maximum channel delay is about 10 ms.

The transmitted signals were spread with m-sequence containing 63 chips. CSK modulation carried 5 bits and MFSK modulation carried 2bits, 3bits and 4bits. The length of the burst frame was 94.5ms. The highest data rate was 317 bps. When capturing the signal, the search frequency range is $f_c - 100Hz \sim f_c + 100Hz$ and the search step is 5 Hz. The time-frequency 2D search relation figure is shown in Fig.13. We can find there is an obvious peak, so we can easily get the time and frequency synchronization. The sea surface was calm in the experiment duration. The transmitter and receiver were relatively immobile. So the searched Doppler frequency shift was zero.

Fig.14 gives one of the maximum likelihood receiver correlation results of CSK and MFSK modulation before decision. We circle shift the correlation results to make the correlation maximum values overlap in the center. The sharper the correlator outputs, the better the demodulation performs. As shown in Fig.14 we can see that there are sharp correlation peaks with CSK and MFSK modulation. The sidelobes are much lower than the peak values. According to the statistical results, the mean BER under 10^{-3} and the highest data rate is 317 bps in the distance of 5 km.

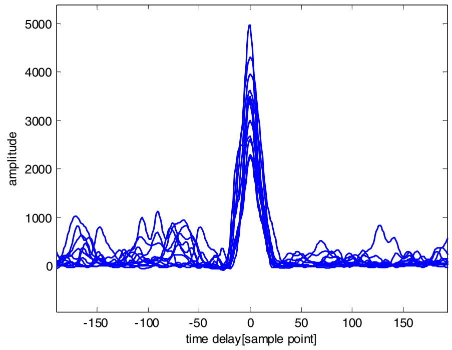

(a) CSK correlation results

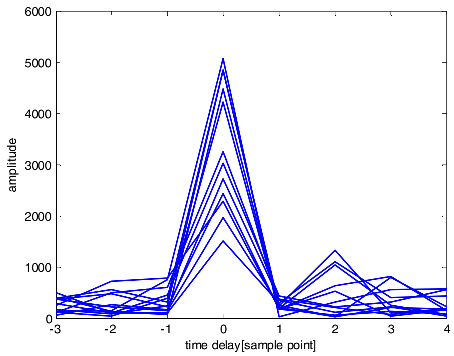

(b) MFSK correlation results

Fig.14 CSK and MFSK correlation results

IV. CONCLUSION

A burst mode hybrid spread spectrum covert acoustic communication is proposed in this paper. It sends extremely short signals randomly and modulates by using the spreading spectrum scheme to realize the covert communication. The hybrid signal contains DSSS-BPSK modulation, CSK modulation and DSSS-MFSK modulation which are modulated by the orthogonal carrier frequency to promote the bandwidth efficiency. This paper provides the self-synchronization scheme and analyzes the performance of the system over the multipath channel. The performance of the proposed system is validated by the shallow water experiment near the South Sea China. In the distance of 5 km, the data rate can achieve up to 317 bps with BER under 10^{-3} over the bandwidth of 4 kHz.

ACKNOWLEDGMENT

This work was supported by the National Natural Science Foundation of China under Grant No. 1127407, National High Technology Research and Development Program of China under Grant No. 2009AA093601-2 and the Underwater Acoustic Technology Laboratory Foundation of China under Grant No. 9140C200801110C2004.

REFERENCES

[1] F. Blackmon, E. Sozer, M. Stojanovic, and J. Proakis, “Performance comparison of RAKE and hypothesis feedback direct sequence spread spectrum techniques for underwater communication applications,” Proceedings of MTS/IEEE OCEARNS’02, vol. 1, 2002, pp. 594-603.

[2] C. C. Tsimenidis, O. R. Hinton, A. E. Adams, and B. S. Sharif, “Underwater acoustic receiver employing direct-sequence spread spectrum and spatial diversity combining for shallow-water multiaccess networking,” IEEE J. Oceanic. Eng., vol. 26, no. 4, pp. 594-603, 2001.

[3] L. L. Yang, “On the study of hybrid DS-SFH spread-spectrum communication system with bandwidth overlapping,” Ph. D. dissertation, Northern Jiaotong Univ., Beijing, China, Apr. 1997.

[4] E. A. Geraniotis, “Coherent hybrid DS/SFH spread-spectrum multiple-access communications,” Special Issue on Militray Communications, IEEE J. Select. Areas Commun., vol. 3, no. 5, pp. 695-705, Sept, 1985.

[5] G. Leus, P. van Walree, J. Boschma. C. Fanciullacci, J. Gerritsen, And P. Tusoni, “Covert underwater communications with multiband OFDM,” OCEANS 2008, Quebec City, Canada, Sept. 2008, pp. 1-8.

[6] P.A. van Walree and G. Leus, “Robust underwater telemetry with adaptive turbo multiband equalization,” IEEE J. Oceanic. Eng., vol. 34, no. 4, pp. 645-655, 2008.

[7] Seong-Bok Park; Dhong-Woon Jang. “A hybrid carrier synchronization scheme for PSK burst-mode communication systems,” 11th International Inference on Advanced Communication Technology, vol. 2, pp. 1357-1360, 2009.

[8] L. Vandendorpe, “Multitone spread spectrum multiple access communications system in a multipath Rician fading channel,” IEEE Trans. on Vehicular Technology, vol. 44, no. 2, pp. 327-337, May 1995.

[9] Yang L.L., Hanzo, L, “Overlapping M-ary Frequency Shift Keying Spread-Spectrum Multiple-Access Systems Using Random Signature Sequences,” IEEE Transactions on Vehicular Technology, vol. 48, no. 6, pp. 1984-1995, 1999.

[10] Zhou F. “The Study of the Key Technologies for Underwater Acoustic Spread-Spectrum Communication,” Ph.D. dissertation, Harbin Engineering Univ., Harbin, China, Dec. 2011.pp. 32-35[周峰．水声扩频通信关键技术研究．哈尔滨：哈尔滨工程大学，2011:32-35.]